

Contents lists available at ScienceDirect

Chemical Engineering Journal

journal homepage: www.elsevier.com/locate/cej





Phosphorus recovery by Donnan dialysis: Membrane selectivity, diffusion coefficients, and speciation effects

Utsav Shashvatt, Fabian Amurrio, Charles Portner, Lee Blaney

University of Maryland Baltimore County, Department of Chemical, Biochemical, and Environmental Engineering, 1000 Hilltop Circle, Engineering Building 314, Baltimore, MD 21250, USA

ARTICLEINFO

Keywords:
Donnan dialysis
Phosphorus
Ion exchange
Nutrient recovery
Circular economy
Resource recovery

ABSTRACT

Donnan dialysis occurs when an electrochemical potential gradient exists for ions on either side of an ionexchange membrane. We posit that this phenomenon can be leveraged to develop a sustainable process for nutrient recovery from wastewater. In this work, we conducted a fundamental study of the key parameters that control orthophosphate (P(V)) removal and recovery by Donnan dialysis. First, a new variable, namely the minimum draw ion concentration ratio between the draw and waste solutions ($R_{d/w}$), was established as the principal design parameter for Donnan dialysis. Then, the following variables were evaluated for their effects on P(V) removal and recovery: waste solution composition; draw anion type and concentration; and, membrane selectivity, thickness, and hydration. The waste solution pH controlled P(V) sorption to the anion-exchange membrane, with HPO_4^{2-} exhibiting a higher affinity than $H_2PO_4^{-}$. For an $R_{d/w}$ of 10, 90.7% of $H_2PO_4^{-}$ and 98.4% of HPO₄⁻⁻ were removed from a 10 mM P(V) waste solution using 100 mN and 218 mN NaCl draw solutions, respectively. The P(V) removal efficiency was dependent on draw solution concentration, and 77.1%, 95.3%, and 98.4% HPO_4^{2-} removal was achieved with 48 ($R_{d/w} = 2$), 115 ($R_{d/w} = 5$), and 218 mM ($R_{d/w} = 10$) NaCl draw solutions, respectively. The rate of P(V) recovery was faster with HCOO⁻ draw anions than with Cl⁻ due to (i) the higher separation factor for P(V) over HCOO- (7.28) compared to Cl- (1.27) and (ii) the greater extent of membrane hydration with HCOO- draw solutions. Overall, this work established a new design parameter $(R_{d/w})$ and applied that parameter to optimize the draw solution chemistry for phosphorus recovery by Donnan dialysis.

1. Introduction

Phosphorus removal and recovery from municipal wastewater and agricultural waste is of paramount importance due to the increasing number of global eutrophication events and growing worldwide food demand [1–3]. Ion exchange-based technologies offer more selective removal and recovery of phosphorus from wastewater than the precipitation-based processes often used during wastewater treatment [4]. Metal (oxy)hydroxide sorbents [5–9], ion-exchange resins [10,11], and hybrid anion exchangers [12,13] have been applied for phosphorus removal from wastewater. These sorbents have a finite capacity that is affected by competition from dissolved organic matter and other more-prevalent anions, leading to variable operational times and performance. Furthermore, pretreatment is needed to remove suspended solids prior to packed-bed sorption columns to avoid maintenance issues. Regeneration of the sorbents requires chemically-intensive

processes that are expensive and produce waste brines that cannot be easily disposed [14]. For these reasons, alternative approaches to phosphorus recovery are needed.

Donnan dialysis with ion-exchange membranes (IEMs) represents a promising solution for phosphorus removal and recovery from wastewater [15]. Unlike ion-exchange resins and metal (oxy)hydroxide sorbents, IEM-based processes do not have capacity constraints, exhibit shorter diffusion pathways, and can be implemented in wastewater containing suspended solids and dissolved organic matter. Donnan dialysis separates chemicals across semi-permeable IEMs placed between waste and draw solutions [16]. It should be noted that electrodialysis operates on similar principles and has been employed for phosphorus removal and recovery from wastewater [17,18]; however, the high ion concentrations, organic matter content, and suspended solids in concentrated waste streams [19] raise key challenges with respect to the energy demand and maintenance of electrodialysis

E-mail address: blaney@umbc.edu (L. Blaney).

^{*} Corresponding author.

systems. Previous Donnan dialysis studies have employed draw solutions composed of monovalent salts (e.g., NaCl) or strong acids (e.g., HCl, HNO₃, H₂SO₄) for anion and cation recovery, respectively [20–22]. For example, Prakash et al. [22] used Donnan dialysis with cation-exchange membranes to recover Al³⁺ and Fe³⁺ from drinking water treatment residuals through exchange reactions with H₃O⁺ from strong acid-based draw solutions. Similarly, Chen et al. [23] demonstrated the feasibility of ammonium recovery from wastewater by Donnan dialysis with a 100 mM NaCl draw solution. We posit that Donnan dialysis can be operated with anion-exchange membranes (AEMs) to recover phosphorus in wastewater using optimized draw solutions containing simple, low-cost, monovalent anions.

In previous efforts, Donnan dialysis has been employed for removal of arsenate [24], chromate [25], fluoride [20], and other anionic contaminants [26,27] from wastewater using chloride-based draw solutions. Trifi et al. [28] reported 68% orthophosphate (P(V)) removal from a 10 mg/L waste solution via Donnan dialysis, and the removal efficiency was improved to 89.5% by adding a calcium alginate adsorbent to the 100 mM NaCl draw solution at pH 12. Although the results of this hybrid system were promising, the need for adsorbents and a high pH draw solution may inhibit implementation. As such, major knowledge gaps exist with respect to draw solution optimization for Donnan dialysis. Hichour et al. [29] and Turki et al. [30] reported the effects of draw ion valence on recovery of nitrate and fluoride, respectively; however, these results were not analyzed or discussed from the perspective of Donnan equilibrium. In addition, the aforementioned studies did not provide a framework to optimize draw solution chemistry for different waste solutions. Hasson et al. [31] evaluated P(V) recovery by Donnan dialysis but only for the H₂PO₄ species. Due to the acid/base chemistry of P(V), multivalent species exist in waste solutions and exhibit different (i) interactions with the AEM and (ii) diffusivities in the AEM. These pHdependent effects have not been systematically investigated for P(V). Moreover, alternate draw anions need to be considered to maximize P (V) transfer from the waste solution to the draw solution. The draw anion valence controls the extent of P(V) recovery by Donnan dialysis, but the draw anion charge density affects P(V) uptake by and diffusion through the AEM. For this reason, monovalent draw anions with variable charge density should be evaluated to optimize P(V) recovery by Donnan dialysis. The membrane affinities for P(V) and the draw anion also require careful consideration to ensure high membrane-phase P(V) concentrations at the interface with the waste solution, which increases the diffusion gradient across the AEM.

The majority of the recoverable phosphorus in wastewater is present as P(V), which exists as the following species: $H_3PO_4^0$; $H_2PO_4^-$; HPO_4^{2-} ; and, PO₄³. The pK_a values for the corresponding acid dissociation reactions are 2.15, 7.20, and 12.38 [32]. Solution pH controls P(V) speciation in the waste and draw solutions; furthermore, the valence on P(V) species affects uptake into the AEM and the overall extent of recovery by Donnan dialysis [33]. Other efforts involving chromate [34] and arsenate [24] treatment by Donnan dialysis did not directly address the uptake and transfer of multivalent, pH-dependent anions across the AEM. This knowledge gap prevents calculation of key parameters required to effectively design Donnan dialysis systems for P(V) removal and recovery from wastewater. For example, the differences in charge density between the four P(V) species suggest distinct affinities to the positively-charged quaternary ammonium functional groups in AEMs. The diffusion coefficients of P(V) species in the AEM vary for related reasons. These species-specific properties complicate efforts to understand P(V) recovery by Donnan dialysis since the monovalent and divalent P(V) species are both relevant to wastewater pH conditions.

The objective of this work was to determine the fundamental parameters that influence P(V) transport through AEMs in order to (1) improve overall understanding of Donnan dialysis and (2) increase P(V) removal and recovery efficiencies. In particular, we investigated the effects of waste and draw solution pH, membrane type and selectivity, and draw solution composition on P(V) removal and recovery. The

waste and draw solution pH control P(V) speciation in the respective solutions, influence P(V) uptake by the AEM, and affect P(V) transport across the membrane. Membrane thickness sets the diffusion pathlength, with thinner membranes providing faster P(V) recovery but lower robustness. The selectivity coefficients control the membrane-phase ion composition at the interfaces with the waste and draw solutions, establish the concentration gradient across the AEM, and, therefore, influence the rate of P(V) recovery. The draw anion and its concentration, valence, diffusion coefficient, and membrane-phase affinity are equally important to the extent and rate of P(V) recovery. To understand the effects of these parameters on P(V) removal and recovery by Donnan dialysis, we conducted experiments with waste solutions buffered at specific pH values to isolate the behavior of the monovalent (H₂PO₄) and divalent (HPO₄²) species. Experimental studies involved two AEMs with different thicknesses and draw solutions comprised of sodium salts of monovalent inorganic (e.g., chloride, Cl⁻) and organic (e.g., formate, HCOO⁻) anions at different concentrations. While the two AEMs were primarily selected for their varying thickness, the inherent chemistry of the membranes also affects other parameters (e.g., selectivity, diffusivity), generating important results for membrane selection in Donnan dialysis applications. The two draw anions were selected to evaluate the impacts of variable charge density on the rate of P(V) recovery. Overall, this work not only establishes the impacts of waste solution composition, membrane properties, and draw solution characteristics on the rate of P (V) removal, but also highlights the technical feasibility of Donnan dialysis for P(V) recovery.

2. Materials and methods

2.1. Chemicals

Unless otherwise stated, all chemicals were obtained from Fisher Scientific (Waltham, MA) or Sigma-Aldrich (St. Louis, MO). Synthetic wastewater solutions were prepared by adding monosodium hydrogen phosphate (NaH2PO4) and disodium hydrogen phosphate (Na2HPO4) to deionized (DI) water. Due to our focus on the fundamental behavior of P (V) in Donnan dialysis, the synthetic wastewater employed in this study did not contain other background anions (e.g., Cl⁻, SO₄², organic matter) present in real wastewater. The 4-morpholineethanesulfonic acid (MES) and 3-(cyclohexylamino)-2-hydroxy-1-propanesulfonic acid (CAPSO) organic buffers were employed to control the pH of the waste and draw solutions. These buffers were used because they exert minimal competition on P(V) interactions with AEMs (see Fig. S1 in the Supporting Information (SI)). Sodium hydroxide (NaOH) was dissolved in DI water to generate 1 M solutions for pH adjustment. Draw solutions were prepared by adding sodium chloride (NaCl) or sodium formate (HCOONa) to DI water. Ion chromatography calibration standards for P (V), Cl⁻, and HCOO⁻ were prepared using 1 g L⁻¹ monoammonium hydrogen phosphate (NH₄H₂PO₄), potassium chloride (KCl), and HCOONa solutions, respectively, from Inorganic Ventures (Christiansburg, VA).

2.2. Anion-exchange membranes

Two AEMs were used in this study, namely AMI-7001 (AMI; Membranes International Inc.; Ringwood, NJ) and FAA-3-PK-130 (FAA; Fumatech BWT GmbH; Germany). These AEMs offered wide pH tolerances (0–10) and high anion-exchange capacities (AECs, 1.3–1.4 meq $\rm g^{-1}$). Both membranes contained quaternary ammonium functional groups. The AECs of the AMI and FAA membranes were confirmed by standard methods (see Text S1–S2 of the SI). The AEMs were selected for their distinct properties, particularly higher hydration (AMI) and lower thickness (FAA); note, membrane hydration was measured using the methods described in Text S3 of the SI. More details on membrane properties are available in Table S1 of the SI.

2.3. Measurement of separation factors

For each AEM, separation factors were calculated for the P(V)-Cland P(V)-HCOO⁻ systems. First, AMI (1 \times 1 cm² or 2 \times 2 cm²) and FAA $(1.5 \times 1.5 \text{ cm}^2 \text{ or } 3 \times 3 \text{ cm}^2)$ coupons were placed in 1 M NaCl or 1 M HCOONa for 24 h to saturate exchange sites with Cl or HCOO, respectively. Membranes were then rinsed with DI water, immersed in fresh 1 M NaCl or 1 M HCOONa for 24 h, and rinsed with DI water. The AEM coupons were then deposited into 250-mL Erlenmeyer flasks containing solutions with total ion concentrations (CT, sum of P(V) and draw ion concentrations) representative of the waste and draw solutions to be used for Donnan dialysis experiments (see Section 2.5). In particular, the tested C_T values were 1, 2, 10, 20, 100, and 218 mN. To ensure that aqueous-phase P(V), Cl-, and HCOO- concentrations were measurable at equilibrium, the smaller coupon sizes were used in solutions with C_T values of 1–2 mN, and the larger AEM coupons were added to the 10–218 mN solutions. The 200-mL solutions were prepared at six different compositions, corresponding to scenarios in which the initial ratio of the P(V) concentration to C_T was 0, 0.2, 0.4, 0.6, 0.8, and 1.0. These experimental solutions were generated by adding appropriate volumes of 10 g L⁻¹ NaH₂PO₄ (as P), Na₂HPO₄ (as P), NaCl, and HCOONa stock solutions to DI water. The mono- and di-sodium phosphate salts were used to generate solutions primarily consisting of the monovalent (pH 4.5-5.2) and divalent (pH 8.6-9.2) P(V) species.

The flasks were sealed with Parafilm and mixed at 250 rpm on an orbital shaker for 24 h to achieve equilibrium. Samples were collected at 0 h (before membrane addition) and 24 h (after membrane addition) for analysis of the P(V), Cl⁻, and HCOO⁻ aqueous-phase concentrations. Note, preliminary experiments demonstrated no change in concentration from 24 h to 48 h of contact (see Fig. S2 in the SI), and so 24 h was deemed appropriate for evaluation of equilibrium conditions. For these binary systems, the P(V) mole fractions in the solution and membrane were calculated with Eq. (1a) and (1b), respectively.

$$x_{P(V)} = \frac{z_{P(V)}C_{P(V)}}{z_{P(V)}C_{P(V)} + z_jC_j}$$
 (1a)

$$y_{P(V)} = \frac{z_{P(V)} \left(C_{P(V),in} - C_{P(V)} \right) V}{AEC \times 10^{-3} \left(m_{dry} \right)}$$
 (1b)

In Eq. 1, $x_{P(V)}$ and $y_{P(V)}$ are the mole fractions (as eq/eq) of P(V) in the solution and membrane, respectively, $z_{P(V)}$ and z_j are the valence of P(V) and Cl^- or HCOO $^-$, respectively, $C_{P(V)}$ and $C_{P(V),in}$ are the equilibrium and initial aqueous-phase P(V) concentrations (mol m $^{-3}$), respectively, C_j is the equilibrium concentration of Cl^- or HCOO $^-$ (mol m $^{-3}$), V is the volume of the solution (m 3), and m_{dry} is the dry mass of the membrane coupon (g).

The mole fractions were used to calculate the separation factor (see Eq. (2), written for the P(V)-A system, where A is a general, monovalent anion).

$$\alpha_A^{P(V)} = \frac{y_{P(V)} x_A}{x_{P(V)} y_A} \tag{2}$$

In Eq. (2), $\alpha_A^{P(V)}$ is the separation factor for P(V) over A, and x_A and y_A are the mole fractions (as eq/eq) of A^- in the solution and membrane, respectively. The separation factors were fit to six experimental measurements using a least squares approach, and the values were reported as mean \pm 95% confidence interval.

2.4. Donnan dialysis reactors

The Donnan dialysis reactors consisted of two 500-mL polycarbonate compartments separated by an AEM. The membrane modules were created by inserting AMI and FAA AEMs between silicon gaskets. Then, the membrane module was placed between the two compartments, and the whole system was secured with stainless steel screws (see Fig. S3 in

the SI). The available membrane surface area was 60 cm².

2.5. P(V) recovery by Donnan dialysis

Based on typical P(V) levels in concentrated waste streams, such as source-separated urine (6–13 mM) [35,36] and animal manure (9–15 mM) [37,38], the P(V) concentration in the synthetic wastewater was set to 10 mM. This P(V) concentration was equivalent to 10 mN and 20 mN for pH conditions where the $\rm H_2PO_4^-$ and $\rm HPO_4^{2-}$ species dominate, respectively. The corresponding draw anion concentration was determined using the ratio of the minimum draw anion concentration in the draw solution ($\rm C_{A,mia}^{draw}$) to the maximum draw anion concentration in the waste solution ($\rm C_{A,max}^{waste}$) for a target P(V) removal efficiency. This ratio was defined as $\rm R_{d/w}$ (Eq. (3)). In Section 3.1, $\rm R_{d/w}$ is established as the principal design variable for Donnan dialysis.

$$R_{d/w} = \left(\frac{C_{A,min}^{draw}}{C_{A,max}^{waste}}\right) \tag{3}$$

Using the fundamental framework developed in Section 3.1, R_{d/w} values of 2, 5, and 10 were chosen for examination of P(V) removal and recovery efficiencies in waste solutions with initial P(V) concentrations of 10 mM. For the three R_{d/w} values, the necessary draw anion (i.e., Cl⁻ or HCOO⁻) concentrations were 20, 50, and 100 mM, respectively, for conditions where H₂PO₄ was dominant and 48, 115, and 218 mM, respectively, for conditions where HPO₄²⁻ was dominant. These calculations are justified in Section 3.1. To conduct these experiments, the pH values of the waste and draw solutions were buffered to 4.0-4.5 (for $H_2PO_4^-$) and 8.5–9.0 (for HPO_4^{2-}) using MES and CAPSO, respectively. For these pH conditions, H₂PO₄ accounts for 98.5–99.4% of P(V) in the MES-buffered solutions, and HPO_4^{2-} constitutes 95.2–98.4% of the P(V) in the CAPSO-buffered solutions; note, the P(V) speciation diagram is provided in Fig. S4 of the SI. The waste and draw solutions were continuously mixed by magnetic stirrer (600 rpm). Sample collection (1mL aliquots) and pH measurements were routinely performed over 100h operational periods and, as needed, small volumes of 1 M NaOH were added to maintain the pH conditions.

To measure the diffusion coefficients of P(V) species, Cl-, and HCOO-, separate Donnan dialysis experiments were performed with an R_{d/w} of 10 for 60-h periods. The aqueous-phase P(V) concentrations in the waste solution were used to calculate the corresponding diffusion coefficients. Diffusion coefficients were calculated from the aggregate data from two experiments, each of which involved 10-12 measurements, and reported as mean \pm standard deviation. During operation, the pH of the draw solutions for the H₂PO₄ experiments was in the 4.8-5.8 range. For the HPO₄²⁻ experiments, the draw solution pH increased from 5.5 to 9.0 within 2 h due to rapid equilibration with the recovered P(V) species and, possibly, HO- migration from the waste solution to the draw solution. As such, the pH gradient between the draw and waste solutions was eliminated for both experimental conditions, isolating transfer of H₂PO₄ and (separately) HPO₄²⁻ across the AEM and enabling calculation of specific diffusion coefficients for $H_2PO_4^-$, HPO_4^{2-} , Cl⁻, and HCOO⁻.

3. Results and discussion

3.1. Theoretical justification of Donnan dialysis for P(V) recovery

3.1.1. Thermodynamic framework for Donnan dialysis

A difference in electrochemical potential for an ion on either side of an AEM prompts the spontaneous exchange reactions central to Donnan dialysis. Fig. 1 highlights the application of Donnan dialysis to recover $H_2PO_4^-$ in wastewater using a draw solution containing a monovalent salt, Na^+A^- . Anions transport across the AEM until electrochemical potential equilibrium is established for the P(V) species and A^- . After

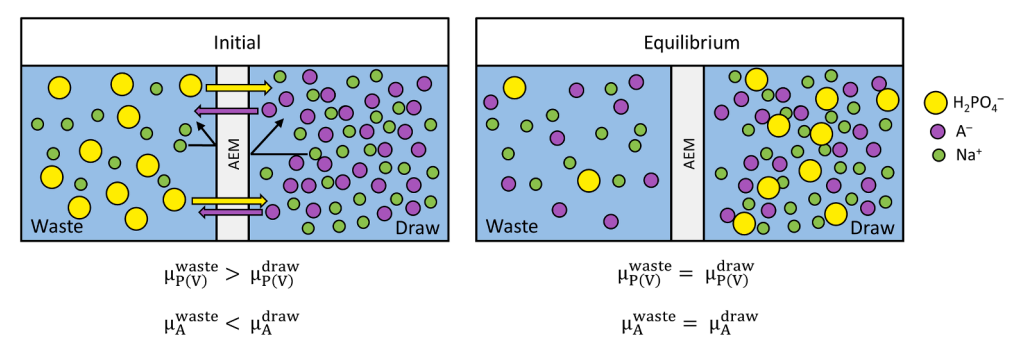


Fig. 1. Schematic showing the exchange of $H_2PO_4^-$, as a representative P(V) species, and A^- , as a general draw anion, through an AEM to achieve Donnan equilibrium.

equating, expanding, and reconfiguring these expressions (see detailed derivation in Text S4 of the SI), Donnan equilibrium can be defined by Eq. (4). Since any of the three P(V) ions (*i.e.*, $H_2PO_4^-$, $H_2PO_4^{2-}$, and PO_4^{3-}) can participate in these exchange reactions, Eq. (4) was written for a general P(V) species.

$$\left(\frac{C_{P(V)}^{draw}}{C_{P(V)}^{waste}}\right)^{\frac{1}{z_{P(V)}}} = k \left(\frac{C_{A}^{draw}}{C_{A}^{waste}}\right)^{\frac{1}{z_{A}}} \tag{4}$$

In Eq. (4), k is a dimensionless constant comprised of the activity coefficients for P(V) and A^- in the waste and draw solutions (see Text S4 in the SI). For Donnan dialysis with 10 mM P(V) waste solutions and draw solutions containing 100 mM and 218 mM A^- , the k terms were equal to 1.00 for $H_2PO_4^-$ and 1.17 for HPO_4^{2-} , respectively (see Table S2 in the SI). It is important to note that while the individual activity coefficients were sensitive to $R_{\rm d/w}$, the aggregate k term exhibited minor variation (i.e., 0.99–1.00 for $H_2PO_4^-$, 1.00–1.19 for HPO_4^{2-}) for $R_{\rm d/w}$ values between 1 and 30.

The $R_{d/w}$ expression from Eq. (3) can be substituted into Eq. (4) to yield Eq. (5).

$$\left(\frac{C_{P(V)}^{draw}}{C_{P(V)}^{waste}}\right) = (k)^{z_{P(V)}} \left(R_{d/w}\right)^{\frac{z_{P(V)}}{z_A}}$$
(5)

According to Eq. (5), the $R_{d/w}$ operating condition controls P(V) recovery since k, $z_{P(V)}$, and z_A are all constant. For an $R_{d/w}$ of 10, the ratio of $H_2PO_4^-$ in the draw solution to $H_2PO_4^-$ in the waste solution was 10, indicating 90.9% recovery; similarly, the HPO_4^{2-} recovery was 99.3% for this $R_{d/w}$ operating condition. This analysis highlights that polyvalent species (e.g., HPO_4^{2-} , PO_4^{3-}) are recovered to a greater extent than monovalent species (e.g., $H_2PO_4^-$) and suggests that Donnan dialysis will be most effective for wastewaters with pH greater than 7.2. Moreover, monovalent draw ions (e.g., CI^- , $HCOO^-$) should be employed to increase P(V) recovery. Prakash and SenGupta [22] reported similar conclusions for recovery of AI^{3+} and Fe^{3+} by Donnan dialysis with cation-exchange membranes and draw solutions containing H_3O^+ .

3.1.2. Donnan dialysis design conditions

The equilibrium concentrations of P(V) and A^- can be defined by mass and charge balances in the waste and draw solutions, as shown in Eq. 6–8; note, these expressions assume no change in the volume of the draw or waste solutions.

$$C_A^{draw} = C_{A, in}^{draw} - \frac{z_{P(V)}}{z_A} C_{P(V)}^{draw}$$

$$\tag{6}$$

$$C_A^{waste} = C_{A,in}^{waste} + \frac{z_{P(V)}}{z_A} C_{P(V)}^{draw} \tag{7}$$

$$C_{P(V)}^{waste} = C_{P(V),in}^{waste} - C_{P(V)}^{draw}$$
(8)

In Eq. 6–8, $C_{A,in}^{draw}$ and $C_{P(V),in}^{waste}$ are the initial aqueous-phase

concentrations (mol m $^{-3}$) of A $^{-}$ and P(V) in the draw and waste solutions, respectively, and $C_{A,in}^{waste}$ is the initial concentration (mol m $^{-3}$) of A $^{-}$ in the waste solution, a term that is ideally 0 to maximize the electrochemical potential gradient across the membrane. After substitution of Eq. 6–8 into Eq. (3) and Eq. (5), $R_{d/w}$ can be expressed as shown in Eq. (9).

$$R_{d/w} = \left(\frac{z_A C_{A, in}^{draw} - z_{P(V)} C_{P(V)}^{draw}}{z_{P(V)} C_{P(V)}^{draw}}\right) = \left(\frac{1}{k}\right)^{z_A} \left(\frac{C_{P(V)}^{draw}}{C_{P(V), in}^{waste} - C_{P(V)}^{draw}}\right)^{\frac{z_A}{z_{P(V)}}}$$
(9)

Eq. (9) can be rearranged to calculate the concentration of recovered P(V) in the draw solution (Eq. (10)) and the required initial concentration of the draw anion in the draw solution (Eq. (11)). These two parameters represent the key outcome and input, respectively, of Donnan dialysis operation.

$$C_{P(V)}^{draw} = \frac{\left(k^{z_A} R_{d/w}\right)^{\frac{z_{P(V)}}{z_A}}}{\left[1 + \left(k^{z_A} R_{d/w}\right)^{\frac{z_{P(V)}}{z_A}}\right]} C_{P(V),in}^{waste}$$
(10)

$$C_{A,in}^{draw} = \frac{Z_{P(V)}}{7} \left(1 + R_{d/w} \right) C_{P(V)}^{draw} \tag{11}$$

Combining Eq. 10–11, the required draw anion concentration can be expressed in terms of $z_{P(V)}$, $R_{d/w}$, and $C_{P(V),in}^{waste}$, as shown in Eq. (12).

$$C_{A,im}^{draw} = \frac{z_{P(V)}}{z_A} \left(1 + R_{d/w} \right) \frac{\left(k^{z_A} R_{d/w} \right)^{\frac{z_{P(V)}}{z_A}}}{\left[1 + \left(k^{z_A} R_{d/w} \right)^{\frac{z_{P(V)}}{z_A}} \right]} C_{P(V),in}^{waste}$$
(12)

This novel expression can be used to determine the necessary draw anion concentration for specific operating conditions (i.e., $R_{d/w}$) that correspond to a target P(V) recovery efficiency from a waste solution with $C_{P(V),in}^{waste}$. Note, Eq. (12) was used to calculate the draw anion concentrations for the experiments described in Section 2.5. Importantly, this same mathematical framework can be applied to other Donnan dialysis systems to recover other ions of interest.

3.1.3. P(V) removal and recovery efficiencies

To validate the relationship derived in Eq. (10), Donnan dialysis experiments were conducted with NaCl-based draw solutions for 100-h periods with $R_{\rm d/w}$ values of 2, 5, and 10 (see Fig. S5 in the SI for experimental data). The experiments were run with the AMI and FAA membranes for pH conditions where $H_2PO_4^-$ and HPO_4^{2-} were the dominant P (V) species (see Fig. S4 of the SI). The removal (Eq. (13)) and recovery (Eq. (14)) efficiencies were calculated using the measured concentrations at 100 h. The P(V) removal efficiency was always greater than the P(V) recovery efficiency (Fig. 2), because a fraction of the P(V) removed from the waste solution remained in the AEM at equilibrium. The fraction of P(V) in the membrane was dependent on the initial P(V) concentration in the waste solution, the initial draw ion concentration, and the AEC of the membrane. For this reason, the following discussion

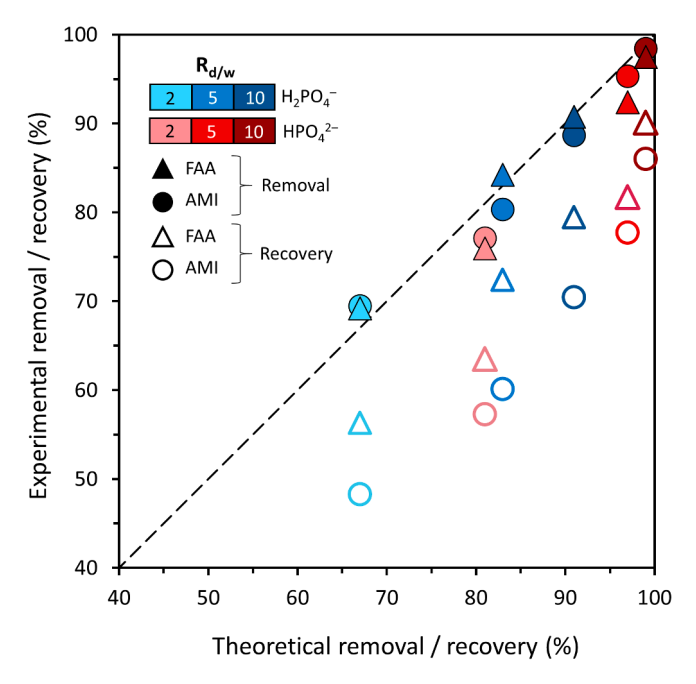


Fig. 2. Experimental and theoretical P(V) removal and recovery efficiencies for variable $R_{\rm d/w}$ operating conditions. The initial P(V) concentration in the waste solution was 10 mM. $\rm H_2PO_4^-$ data stem from waste and draw solutions maintained at pH 4.0–4.5 with 10 mM MES; similarly, the HPO_4^- data were collected from experiments maintained at pH 8.5–9.0 with 10 mM CAPSO. As needed, 1 M NaOH was dosed to maintain pH conditions. The draw solutions were composed of 20 and 48 mM NaCl ($\rm R_{d/w}=2$), 50 and 115 mM NaCl ($\rm R_{d/w}=5$), and 100 and 218 mM NaCl ($\rm R_{d/w}=10$) for the $\rm H_2PO_4^-$ and $\rm HPO_4^{2-}$ systems, respectively. Donnan dialysis was performed for 100 h.

primarily focuses on P(V) removal efficiency to avoid unfair comparisons of recovery efficiency between operating conditions. It is important to note that continuous-flow Donnan dialysis configurations will exhibit P(V) recovery efficiencies that are more similar to the P(V) removal efficiency, because a smaller fraction of the removed P(V) will remain in the membrane as the volume of treated wastewater increases.

$$\eta_{removal} = \left(1 - \frac{C_{P(V)}^{waste}}{C_{P(V),in}^{waste}}\right) \tag{13}$$

$$\eta_{recovery} = \left(\frac{C_{P(V)}^{draw}}{C_{P(V),im}^{waste}}\right) \tag{14}$$

The experimental results in Fig. 2 show that $R_{d/w}$ values of 2, 5, and 10 provided 68.9–69.2%, 80.3–84.2%, and 88.6–90.7% P(V) removal at pH 4.0-4.5 (H₂PO₄ dominant species) and 75.9-77.1%, 92.3-95.3%, and 97.5–98.4% P(V) removal at pH 8.5–9.0 (HPO $_4^{2-}$ dominant species). The experimental removal efficiencies were in agreement with the theoretical removal efficiencies predicted by Eq. (13). As explained above, the experimental recovery efficiencies were lower than the removal efficiencies, because a fraction of the P(V) remained in the membrane phase after 100 h of Donnan dialysis. The percent of the total P(V) in the membrane phase was 12.4-21.1% for the thicker AMI membranes and 7.4-12.9% for the thinner FAA membranes. The lower and higher bounds of these ranges corresponded to $R_{\text{\tiny d/w}}$ values of 10 and 2, respectively. This result was expected because higher Cl^- concentrations decrease the P(V) content in the membrane through competition effects. Osmosis resulted in a minor amount of water transport from the waste solution to the draw solution. For experiments with the AMI membranes, the waste and draw solution volumes changed by 0.2-4.5% and 0.6-5.7%, respectively; the corresponding volume changes were 0.2-1.6% and 4.1-5.1%, respectively, with the FAA membranes. Therefore, osmosis had a minimal effect on P(V) removal and recovery.

To ensure high P(V) removal efficiencies, $R_{\text{d/w}}$ was set to 10 for most of the experiments described below.

3.2. Factors affecting the selective uptake of P(V) species by AEMs

The composition of the waste and draw solutions affects the membrane selectivity coefficients and separation factors for the P(V)-draw ion system. These two ion-exchange parameters depend on the total ion concentration in the solution, the valence of the P(V) species, membrane characteristics, and the specific draw ion [39]. The effects of these four properties on the separation factor are explored in greater detail below. A separation factor greater than 1.0 signifies that the AEM prefers P(V) over the draw ion, with higher separation factors indicating higher P(V) content in the membrane phase. Separation factors provide a fairer comparison of P(V) species due to the inherent differences in the selectivity coefficient expressions for monovalent-monovalent exchange reactions (e.g., the H₂PO₄-A⁻ system) and divalent-monovalent exchange reactions (e.g., the HPO₄²-A⁻ system). The effective separation factors for P(V) over A⁻ $\left(\alpha_A^{P(V)}\right|_{\text{eff}}\right)$ can be calculated according to Eq. (15), which was derived in Text S5 of the SI.

$$\left. \alpha_A^{P(V)} \right|_{eff} = \left(\frac{q_{tot,P(V)}}{C_{tot,P(V)}} \right) \left(\frac{C_A}{q_A} \right) \tag{15}$$

In Eq. (15), $q_{tot,P(V)}$ is the total membrane-phase concentration of P(V) (mol m $^{-3}$), and $C_{tot,P(V)}$ is the total aqueous-phase concentration of P(V) (mol m $^{-3}$). In this study, $\alpha_A^{P(V)}\Big|_{eff}$ was calculated at pH 4.5 and 9.0 and used to define $\alpha_A^{H_2PO_4^-}$ and $\alpha_A^{HPO_4^2}$, respectively. These two parameters can be used to predict separation factors at other environmentally-relevant pH conditions (see Fig. S6 of the SI).

The measured separation factors varied with C_T , as indicated in Fig. 3 and Table 1; note, the isotherms for all conditions are provided in Figs. S7-S18 of the SI. For the two membranes (i.e., AMI, FAA) and two draw anions (i.e., Cl^- , $HCOO^-$), the separation factors varied as follows: 0.05-4.82 for $H_2PO_4^-$ and 0.18-25.87 for HPO_4^{2-} at low C_T (1 and 2 mN, respectively); 0.21-2.26 for $H_2PO_4^-$ and 0.75-7.28 for HPO_4^{2-} at medium C_T (10 and 20 mN, respectively); and, 0.51-1.13 for $H_2PO_4^-$ and 0.81-1.86 for HPO_4^{2-} at high C_T (100 and 218 mN, respectively). These data indicate that separation factors are highest in solutions with low C_T values and converge to 1 at higher C_T . The affinity of AEM sites for P(V) should, therefore, be higher in the low C_T conditions that exist in the waste solution. In the high C_T draw solution, the separation factors are expected to be closer to 1. These separation factors are important because they set the boundary conditions for P(V) concentrations in the AEM and control the rate of Fickian diffusion across the membrane.

As indicated in Fig. 3, the HPO $_4^{2-}$ species exhibited greater separation factors than ${\rm H_2PO_4^-}$ with the Cl⁻ and HCOO⁻ draw ions. This result was expected because the higher charge density of HPO $_4^{2-}$ leads to a higher affinity for the quaternary ammonium functional groups in the AEMs, as observed for other ions [40]. The higher separation factors observed for the AMI membrane increased the membrane-phase P(V) concentrations at the waste solution interface compared to those for the FAA membrane. Because the draw solution separation factors converge to 1 for all conditions, a higher membrane-phase P(V) concentration at the waste solution interface increases the P(V) concentration gradient in the membrane (see Fig. S19 of the SI). These conditions should increase the rate of P(V) recovery in the AMI membranes; however, other factors (e. g., diffusion coefficient, membrane thickness) also influence the rate of P (V) removal. The cumulative effects of these parameters on P(V) flux is discussed in Section 3.5.

The greater magnitude of $\alpha_{HCOO^-}^{P(V)}$ compared to $\alpha_{Cl^-}^{P(V)}$ indicated that P (V) is more competitive against HCOO $^-$ than against Cl $^-$, particularly at low and medium C_T. These results can be attributed to the impacts of draw ion hydration and charge density on ion affinity [41]. The non-

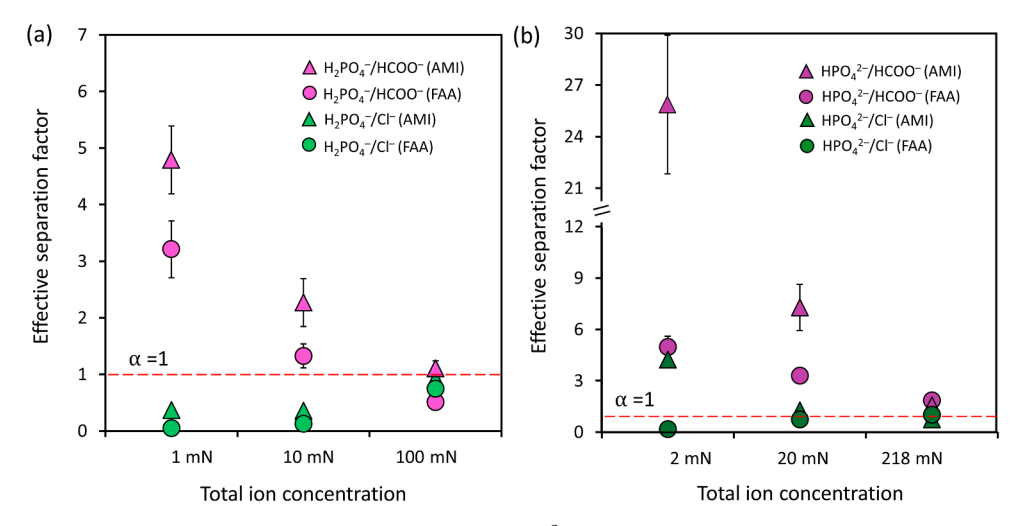


Fig. 3. Effective separation factors for (a) monovalent $H_2PO_4^-$ and (b) divalent HPO_4^{2-} over Cl^- and $HCOO^-$ for the AMI and FAA AEMs. The membranes were initially in the Cl^- or $HCOO^-$ form. The pH of the solutions in (a) and (b) were in the range of 4.3–5.5 and 8.8–9.5, respectively. The solutions were continuously mixed on an orbital shaker at 150 rpm for 24 h.

hydrated ionic radii of HCOO $^-$ (1.8–1.9 Å) and Cl $^-$ (1.8 Å) are similar [42]; however, the median hydration number (from available literature) of HCOO $^-$ (5.5) is greater than Cl $^-$ (3.7) [43–47]. Therefore, HCOO $^-$ undergoes greater hydration and exhibits a lower charge density than Cl $^-$, resulting in less competition for interaction with the quaternary ammonium groups of the AMI and FAA membranes. This result was also confirmed by the higher degree of hydration measured for both AMI and FAA membranes when submerged in HCOONa solutions compared to those immersed in NaCl solutions (see Table S1 of the SI). Teppen *et al.* reported similar observations with cations of equal valence [48]. To confirm this point, the $\alpha^{\text{Cl}^-}_{\text{HCOO}^-}$ values were calculated for all conditions (not shown) and found to be consistently greater than one. The outcomes of these experiments indicate that small organic anions may serve as better draw anions than Cl $^-$ in Donnan dialysis operations.

3.3. Transport of mono- and di-valent P(V) species in Donnan dialysis

The rate of P(V) removal from the 10 mM waste solution was limited by P(V) transport through the AEM via Fickian diffusion and electromigration. The P(V) flux through the membrane was modeled using the Nernst-Planck equation (Eq. (16)).

$$\overline{J}_{P(V)} = -D_{P(V)} \left[\frac{dq_{P(V)}}{dx} + \frac{z_{P(V)}q_{P(V)}F}{RT} \left(\frac{d\emptyset}{dx} \right) \right]$$
(16)

In Eq. (16), \bar{J} (mol m⁻² min⁻¹) is the flux, D (m² min⁻¹) is the diffusion coefficient, R is the universal gas constant, T is the temperature, F is the Faraday constant, \varnothing is the electric potential of the solution, and x is the distance into the membrane.

Following a series of mathematical steps and substitutions, which are comprehensively detailed in Text S6 of the SI, Eq. (16) was converted into an expression for the rate of P(V) removal in the waste solution in terms of known (i.e., $z_{P(V)},\ z_A,\ L,\ V,\ Q,\ \alpha_W,\ \alpha_D,\ C_{P(V)}|_W,\ C_T^{waste},\ C_T^{draw},\ C_{P(V),in}^{waste})$ and modeled (i.e., $D_{P(V)},\ D_A)$ parameters (Eq. (17)). The analytical expression was a large nested function and was not included here for the sake of brevity.

Table 1Summary of parameters for P(V), Cl⁻, and HCOO⁻ transport by Donnan dialysis.

J 1		, ,
Parameter	Value	
Design / operational		_
V (m ³)	5.0×10^{-4}	
S (m ²)	$6.0 imes 10^{-3}$	
$C_T^{\text{waste}}(\text{eq m}^{-3})$	10 or 20	
$C_T^{draw}(eq m^{-3})$	100 or 218	
$C_{P(V),in}^{waste} (mol m^{-3})$	10	
Membrane-specific	AMI	FAA
L (HCOO ⁻ form) (m) ^a	$(6.3 \pm 0.1) \times 10^{-4}$	$(1.1 \pm < 0.1) \times 10^{-4}$
L (Cl ⁻ form) (m) ^a	$(5.7 \pm 0.1) \times 10^{-4}$	$(0.9 \pm < 0.1) \times 10^{-4}$
Q (HCOO $^-$ form) (eq m $^{-3}$)	$1.38 imes 10^3$	1.40×10^{3}
Q (Cl ⁻ form) (eq m ⁻³)	1.72×10^{3}	1.52×10^{3}
$D_{H_2PO_4^-}(m^2 min^{-1})^b$	$(2.5\pm0.6)\times10^{-10}$	$(8.0 \pm 1.3) \times 10^{-11}$
$D_{HPO_4^{2-}}(m^2 min^{-1})^b$	$(2.1\pm0.1)\times10^{-10}$	$(3.5\pm0.7)\times10^{-11}$
$D_{Cl^{-}}(m^2 min^{-1})^{b}$	$(6.7 \pm 0.3) \times 10^{-9}$	$(4.8 \pm 1.5) \times 10^{-10}$
$D_{HCOO^{-}}(m^2 min^{-1})^{b}$	$(9.0 \pm < 0.1) \times 10^{-9}$	$(8.8\pm1.1)\times10^{-10}$

a: Thickness and standard deviation calculated from three replicates.

In Eq. (17), S is the membrane surface area (m²), L is the hydrated membrane thickness (m), V is the volume of the waste and draw solutions (equivalent in this study, m³), Q is the anion-exchange capacity (eq m⁻³), α_W and α_D are the separation factors at the membrane interfaces with the waste and draw solutions, respectively, and $C_{P(V)}\big|_W$ is the membrane-phase P(V) concentration at the interface of the waste solution.

Eq. (17) was solved using the Runge-Kutta numerical method in Matlab. In the mathematical analysis, a number of common assumptions were avoided to attain a more comprehensive, universal, and accurate model. For example, the diffusion coefficient of the P(V) ion was not equated to that of the draw ion (as in Hasson *et al.* [49]) and the draw ion diffusion coefficient was not neglected (as in Zhao *et al.* [50]). In

$$\frac{dC_{P(V)}\mid_{W}}{dt} = \operatorname{fn}\left(z_{P(V)}, z_{A}, D_{P(V)}, D_{A}, S, L, V, Q, \alpha_{W}, \alpha_{D}, C_{P(V)}\mid_{W}, C_{T}^{waste}, C_{T}^{draw}, C_{P(V), in}^{waste}\right)$$

$$(17)$$

b: Diffusion coefficient and standard deviation calculated from duplicate experiments.

previous models reported by Miyoshi *et al.* [51] and Agarwal *et al.* [52], the membrane-phase ion concentration was assumed to be negligible; however, this assumption is not valid for some $R_{\rm d/w}$ operating conditions, as indicated by the differences in removal and recovery efficiencies from Fig. 2. Importantly, the use of separation factors allowed derivation of an expression that applies to all P(V) species. Previous researchers have used selectivity coefficients to derive expressions similar to Eq. (17) for monovalent and divalent ions, but the derivations become mathematically complex for trivalent ions [53]. The separation factor-based expression in Eq. (17) can be employed for $H_2PO_4^-$, $HPO_4^2^-$, or PO_4^{3-} and, therefore, represents an effective tool to model P(V) transport in diverse Donnan dialysis applications.

The rate of P(V) removal from the waste solution was governed by the following operational parameters: initial P(V) concentration in the waste solution; C_T values of the waste and draw solutions; membrane capacity, thickness, and surface area; and, waste and draw solution volume. The values of these parameters for the Donnan dialysis system used in this study are reported in Table 1. In addition, parameters related to membrane chemistry also play a crucial role in the rate of P(V) removal from the waste solution. These parameters include (i) separation factors for P(V) species over draw ions (e.g., Cl^- , $HCOO^-$) in the waste and draw solutions and (ii) diffusion coefficients for the individual P(V) species and draw ions in the AEM. The separation factors were reported in Fig. 3. Using the operational parameters and measured separation factors, the diffusion coefficients were determined by fitting the experimental P(V) concentration data to Eq. (17). The calculated diffusion coefficients are reported in Table 1.

Overall, the rates of removal for $H_2PO_4^-$ and HPO_4^{2-} were higher when HCOO was used as the draw ion (see Fig. 4). The mean initial rates of removal for $H_2PO_4^-$ and HPO_4^{2-} in the AEMs were (2.4 \pm 0.1) \times 10^{-2} and (1.2 \pm 0.2) \times 10^{-2} mol m^{-3} min $^{-1}$, respectively, with the $HCOO^-$ draw ion; additionally, the initial rates of removal for $H_2PO_4^$ and HPO $_4^{2-}$ were (1.3 \pm 0.1) \times 10 $^{-2}$ and (8.4 \pm 2.3) \times 10 $^{-3}$ mol m $^{-1}$ min⁻¹, respectively, for the Cl⁻ draw ion. The initial rate of H₂PO₄⁻ removal was almost 2 \times that of HPO₄²⁻ due to the 2 \times uptake of monovalent species (compared to divalent species) by the AEM. Draw solutions with HCOO provided as much as 85% faster P(V) removal compared to draw solutions comprised of Cl due to the higher separation factor for P(V) against HCOO⁻, which resulted in a greater P(V) concentration gradient in the AEM. The diffusion coefficients for H₂PO₄ and HPO₄²⁻ in the FAA membrane were (8.0 \pm 1.3) \times 10⁻¹¹ and (3.5 \pm 0.7) $\times\,10^{-11}\,\text{m}^2\,\text{min}^{-1},$ respectively; likewise, the diffusion coefficients for $H_2PO_4^-$ and HPO_4^{2-} in the AMI membrane were (2.5 \pm 0.6) \times 10^{-10}

and (2.1 \pm 0.1) \times 10^{-10} m² min $^{-1}$, respectively. The higher charge density of HPO $_4^2$ compared to $H_2PO_4^-$ resulted in stronger binding with quaternary ammonium exchange sites, thereby reducing the diffusivity of HPO $_4^2$ in the AEM. This result differs from the findings of Zhao $\it{et~al.}$ [50], who reported faster removal of HAsO $_4^2$ than $H_2AsO_4^-$ by Donnan dialysis for a waste stream containing 15 μM As(V) and 10 mM NaCl and a draw solution with 100 mM NaCl. These contrasting results likely stem from the lower As(V) concentration in the waste solution, raising important insight into differences in Donnan dialysis systems aimed at trace contaminant treatment and resource recovery from more concentrated waste streams.

The calculated diffusion coefficient of HCOO $^-$ [(8.8 \pm 1.1) imes 10 $^{-10}$ $\text{m}^2 \, \text{min}^{-1}]$ was 83% greater than that of Cl $^-$ [(4.8 \pm 1.5) \times $10^{-10} \, \text{m}^2$ min⁻¹] for FAA, highlighting the benefits of using small organic anions in draw solutions. Similarly, the diffusion coefficient for HCOO $^-$ [(9.0 \pm $<0.1) \times 10^{-9} \, \text{m}^2 \, \text{min}^{-1}$] was 34% greater than that of Cl⁻ [(6.7 \pm 1.3) \times 10⁻⁹ m² min⁻¹] in the AMI membrane. Interestingly, the faster diffusivity of HCOO⁻ in the AEM contrasts with the diffusion coefficients of Cl⁻ $(1.2 \times 10^{-7} \text{ m}^2 \text{ min}^{-1} \text{ at } 25 \text{ °C } [54])$ and HCOO⁻ $(8.46 \times 10^{-8} \text{ m}^2 \text{ m}^2$ min⁻¹ at 25 °C [55]) in water. However, the magnitude and order of the calculated diffusion coefficients in the AEM agree with previous studies. For example, Mazrou et al. [56] and Akgemci et al. [57] reported the diffusion coefficients of Cl $^-$ and HCOO $^-$ to be $6.03 \times 10^{-10}~\text{m}^2~\text{min}^{-1}$ and 1.9 \times $10^{-9}\,\text{m}^2\,\text{min}^{-1}$, respectively, in the Neosepta ACM membrane. Note, a larger (more hydrated) monovalent anion (e.g., HCOO⁻) exerts more swelling potential, leading to an increase in intermolecular spacing in the AEM, than a smaller (less hydrated) monovalent anion (e.g., Cl⁻) because the number of moles of both anions has to be equivalent to maintain electroneutrality in the membrane. Therefore, the ion mobility within the AEM was higher for the HCOO⁻ system.

The difference in the ratio of the diffusion coefficient of HCOO⁻ over that of Cl⁻ in the FAA and AMI membranes might stem from the extent of membrane hydration. The AMI membrane was more hydrated and, therefore, exhibited less specificity between the two draw ions [58–61], whereas FAA was less hydrated and resulted in higher diffusivity for the more hydrated (*i.e.*, lower charge density) HCOO⁻ ion. These effects can be observed in Fig. 4. Although the greater extent of hydration in the AMI membrane enabled faster ion diffusion, the increased thickness of the AMI membranes resulted in a lower P(V) concentration gradient which, ultimately, reduced P(V) flux (Fig. S19 of the SI). It is important to note that the overall P(V) recovery at Donnan equilibrium should be similar for both draw anions (see Eq. (14), after substitution of Eq. (10)); however, the faster rate of P(V) removal is an important design

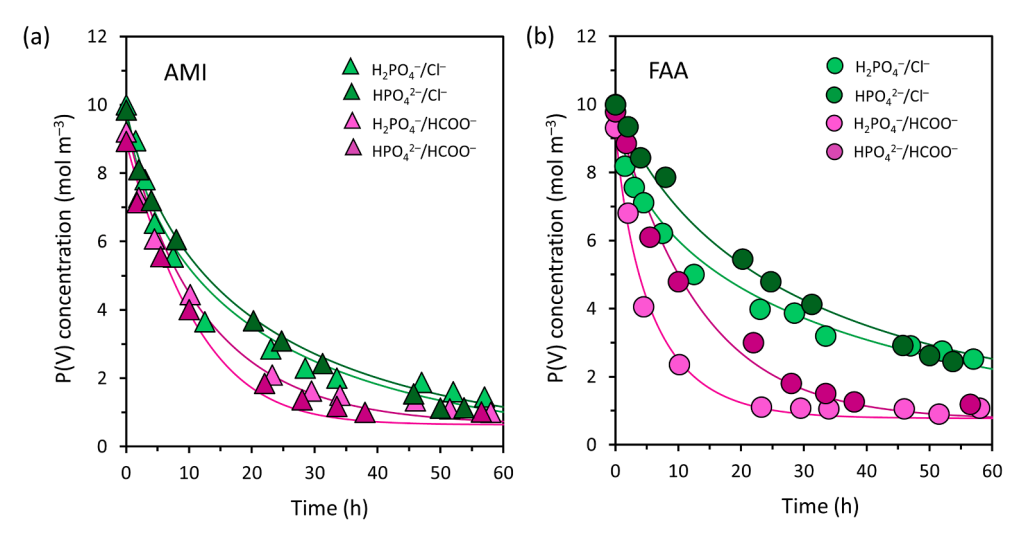


Fig. 4. Time-dependent concentration profiles of P(V) in the waste solution for Donnan dialysis with Cl^- and $HCOO^-$ draw solutions and (a) AMI and (b) FAA membranes. The pH values of the waste and draw solutions in the $H_2PO_4^-$ - A^- and $HPO_4^2^-$ - A^- systems were maintained at 4.5–5.0 and 8.5–9.0, respectively. The $R_{d/w}$ was 10 for all conditions. Solutions were continuously mixed at 600 rpm on a magnetic stirring station.

consideration for high-throughput Donnan dialysis systems.

3.4. Effect of $R_{d/w}$ on the rate of P(V) removal in Donnan dialysis

The rate expression for P(V) removal from the waste solution (Eq. (17)) was reconfigured to be a function of $R_{d/w}$ (Eq. (18)), following the steps documented in Text S6 of the SI.

$$\frac{dC_{P(V)}|_{W}}{dt} = \text{fn} \left(z_{P(V)}, z_{A}, D_{P(V)}, D_{A}, S, L, V, Q, \alpha_{W}, \alpha_{D}, \eta_{\text{removal}}, R_{d/w}, C_{P(V), \text{in}}^{\text{waste}} \right)$$
(18)

For a design $\eta_{\text{removal}},$ Eq. (18) can be solved for the rate of P(V) removal from the waste solution as a function of $R_{d/w}$. Eq. (14) (after substituting Eq. (10)), Eq. (12), and Eq. (18) were solved for $R_{d/w}$ values of 1-30 to determine the recovery efficiency, required draw ion concentration, and rate of removal, respectively, for both H₂PO₄ and HPO_4^{2-} (Fig. 5). One important conclusion from Fig. 5 is that $R_{d/w}$ had a negligible impact on the rate of removal, which was measured at $\eta_{removal}$ = 0.1. Rather, the rate of removal was more dependent on the P(V) concentration gradient in the membrane. In the initial stage of Donnan dialysis, the P(V) concentration gradient in the membrane is determined by $C_{P(V)}^{\text{waste}}$ and α_W ; therefore, the rate is independent of the draw solution composition and, hence, $R_{d/w}$. For high $R_{d/w}$ operating conditions, α_D goes to 1, and the membrane-phase P(V) concentration at the interface with the draw solution will be low. For these reasons, $R_{d/w}$ does not affect the initial rate of P(V) removal. This conclusion was experimentally confirmed for R_{d/w} values of 5, 10, and 50 (see Fig. S21 of the SI) and reinforced by a sensitivity analysis to determine the impact of $\alpha_{\!D}$ on the rate of P(V) removal (see Section 3.5). It is important to note that the rates of removal for H₂PO₄ and HPO₄² were sensitive to other parameters, such as membrane properties (e.g., membrane capacity, thickness, and hydration), α_W , and the diffusion coefficients of P(V) species and draw ions (see Section 3.5).

3.5. Sensitivity analysis of operational and fundamental parameters on the initial rate of P(V) removal by Donnan dialysis

Eq. (18) was used to assess the sensitivity of the initial rate of H_2PO_4

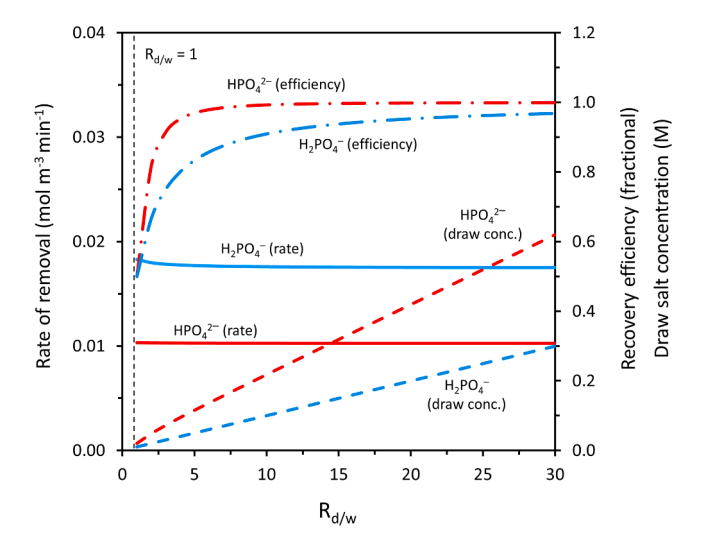


Fig. 5. The P(V) recovery efficiency, initial rate of P(V) removal, and required salt concentration in the draw solution as a function of $R_{\rm d/w}$. These relationships correspond to an initial P(V) concentration of 10 mM in the waste solution. Removal efficiencies, draw ion concentrations, and removal rates were calculated using Eq. (14) (after substituting Eq. (10)), Eq. (12), and Eq. (18), respectively. The rate of removal curves stem from average data from four experimental conditions that employed different membranes and draw ions.

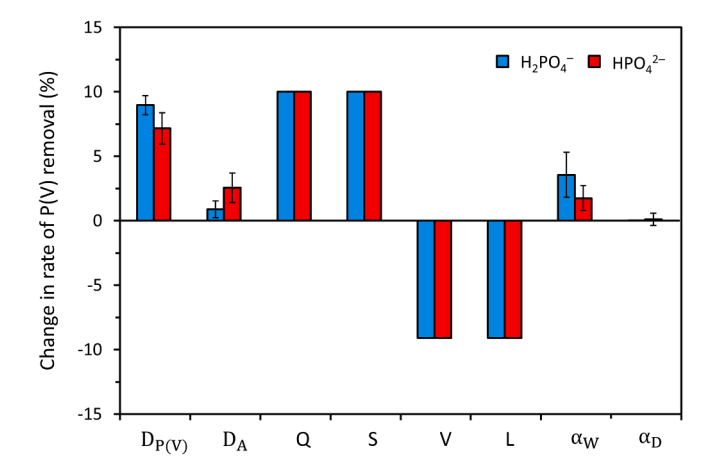


Fig. 6. Sensitivity analysis on the initial rate of P(V) removal for a 10% increase in the listed parameters. The initial rate of P(V) removal was calculated for $\eta_{removal}=0.1.$ The base values for each parameter are shown in Table 1.

and HPO $_4^{2-}$ removal to the following operational and fundamental parameters: P(V) and draw ion diffusion coefficients; separation factors in the draw and waste solutions; membrane properties, such as thickness and density of anion-exchange sites; and, reactor-specific parameters, such as volume and membrane surface area. Note, some of these parameters are dependent on each other and, therefore, cannot be exclusively controlled (e.g., a change in the density of anion-exchange sites will also affect the diffusion coefficient). Nevertheless, this analysis determined which system variables had the greatest and least impacts on P(V) removal rate.

Fig. 6 shows that the rate of P(V) removal was more sensitive to a 10% change in P(V) diffusion coefficient (7.2-8.9%) than a 10% change in draw ion diffusion coefficient (0.2-2.6%). From an operational standpoint, it is more convenient to employ different draw ions with higher diffusion coefficients; however, the above findings suggest that fabrication of AEMs with higher P(V) diffusivity will lead to greater improvements in the rate of P(V) removal. Hasson et al. [31] alluded to the same result but did not present experimental data to confirm this finding. With respect to separation factors, a 10% change in α_D had a negligible effect on P(V) removal rate (~0.01%); however, a 10% increase in α_W improved the rate of P(V) removal (1.8–3.5%). This result was expected because the α_W separation factor directly controls the P(V) concentration gradient in the membrane (see Fig. S19 in the SI). Based on these findings, it may be acceptable to assume that $\alpha_D=1$ in Donnan dialysis systems operating at high $R_{d/w}$. A 10% increase in Q had a strong impact on the rate of P(V) removal (10%) due to greater P(V) uptake by the membrane. A 10% change in membrane thickness almost proportionally changed the rate of P(V) removal (9%) due to linear effects on the concentration gradient in the AEM. The impact of reactor configuration parameters, such as reactor volume or membrane surface area, were not experimentally evaluated, but these parameters are expected to have a proportional impact on the rate of P(V) removal based on Eq. (18). The results of the sensitivity analysis indicated that fundamental factors, such as higher membrane selectivity for P(V) and faster diffusion of P(V) in the membrane, can further improve P(V) recovery by Donnan dialysis. Overall, this information, along with the experimental data reported above, will enable future technoeconomic assessments to compare the performance and cost of Donnan dialysis systems to other technologies.

4. Conclusion

This study provided, for the first time, a conceptual framework for the equilibrium and kinetic aspects of Donnan dialysis-based P(V) removal and recovery. A new parameter, $R_{\rm d/w}$, was established as the

primary design variable for achieving targeted P(V) removal and recovery efficiencies. The main advantage of this parameter is that it is independent of the P(V) concentration in the waste solution and can be broadly applied to different systems. Overall, the equilibrium P(V) removal efficiency was found to be dependent on three main parameters: P(V) valence; draw anion valence; and, $R_{d/w}$. For the same $R_{d/w}$ condition, higher recovery efficiencies were obtained for HPO₄²⁻ than H₂PO₄. According to the derived expressions, monovalent draw ions (e. g., Cl⁻, HCOO⁻) enable greater P(V) removal than polyvalent anions. A higher R_{d/w} can be achieved by increasing the salt concentration in the draw solution, conditions that enhanced the P(V) removal and recovery efficiencies. However, this strategy involves diminishing returns when $R_{d/w}$ exceeds 10. At this operating condition, removal efficiencies of up to 90.7% for $H_2PO_4^-$ and 98.4% for HPO_4^{2-} were achieved using NaCl as the only chemical input. Importantly, the experimental measurements closely matched theoretical expectations.

The rate of P(V) removal was determined to be a function of the P(V) speciation, separation factors for the P(V) species over the draw anion. diffusion coefficients of P(V) species and draw anions, and membrane properties. The separation factor of P(V) over the draw anion was strongly influenced by the P(V) valence, the C_T of the waste and draw solutions, and the draw anion type. For the tested conditions, the separation factors for H₂PO₄ and HPO₄² over HCOO were both greater than 1, but the AEMs exhibited a higher affinity for the divalent P(V) species. Interestingly, the separation factors for $H_2PO_4^-$ and HPO_4^{2-} over Cl were<1, indicating less selective P(V) uptake in the presence of prevalent inorganic anions at the tested conditions. Due to the high C_T maintained in the draw solution, the separation factor at the membrane interface with the draw solution was approximately 1.0 for all tested conditions. On the other hand, the separation factor at the membrane interface with the waste solution was highly dependent on the P(V) valence, draw anion, and membrane characteristics. The two separation factors set the P(V) concentration gradient in the AEM and, thereby, controlled P(V) flux through the membrane. The P(V) flux also depends on diffusion coefficients for P(V) and the draw anion. The diffusion coefficient of $H_2PO_4^-$ was similar to or greater than that of HPO_4^{2-} , depending on AEM properties. Membrane properties, such as hydration and thickness, strongly impacted the rate of P(V) recovery. In general, higher membrane hydration increased the diffusion coefficients and thicker membranes lowered the diffusion gradient.

In this study, optimal P(V) recovery by Donnan dialysis was achieved using the FAA membrane and a $HCOO^-$ draw anion at pH conditions that favor the presence of $H_2PO_4^-$. Overall, the results provided novel insight into opportunities to design, optimize, and apply Donnan dialysis systems. These insights will enable application of Donnan dialysis for phosphorus recovery from municipal wastewater, source-separated urine, animal manure, and other nutrient-rich waste streams. The next steps to scale-up of Donnan dialysis processes will require (i) performance evaluation in real waste streams that contain high levels of competing anions, dissolved organic matter, and suspended solids and (ii) development of unique membrane configurations that increase the surface area-to-volume ratio and improve the overall rate of recovery.

Declaration of Competing Interest

The authors declare that they have no known competing financial interests or personal relationships that could have appeared to influence the work reported in this paper.

Acknowledgements

We gratefully acknowledge funding from NSF CBET-1706819. We would also like to acknowledge Mr. Victor Fulda for his technical help with fabrication of the Donnan dialysis reactors.

Appendix A. Supplementary data

Supplementary data to this article can be found online at https://doi. org/10.1016/j.cej.2021.129626.

References

- [1] S.B. Bricker, B. Longstaff, W. Dennison, A. Jones, K. Boicourt, C. Wicks, J. Woerner, Effects of nutrient enrichment in the nation's estuaries: A decade of change, Harmful Algae 8 (1) (2008) 21–32.
- [2] J. Cooper, R. Lombardi, D. Boardman, C. Carliell-Marquet, The future distribution and production of global phosphate rock reserves, Resour. Conserv. Recycl. 57 (2011) 78–86.
- [3] State-EPA Nutrient Innovation Task Group, An Urgent Call to Action Report of the State-EPA Nutrient Innovation Task Group, 2009. https://www.google.com/url?sa=t&rct=j&q=&esrc=s&source=web&cd=&ved=2ahUKEwi178Tq-u7vAh WbFFkFHRKTA1IQFjAAegQIBhAD&url=https%3A%2F%2Fwww.epa.gov%2Fsites%2Fproduction%2Ffiles%2Fdocuments%2Fritgreport.pdf&usg=AOvVaw22TgA7tn6EAzI8MnBJDHwc.
- [4] G. Morse, S. Brett, J. Guy, J. Lester, Phosphorus removal and recovery technologies, Sci. Total Environ. 212 (1998) 69–81.
- [5] S. Tanada, M. Kabayama, N. Kawasaki, T. Sakiyama, T. Nakamura, M. Araki, T. Tamura, Removal of phosphate by aluminum oxide hydroxide, J. Colloid Interface Sci. 257 (1) (2003) 135–140.
- [6] K. Karageorgiou, M. Paschalis, G.N. Anastassakis, Removal of phosphate species from solution by adsorption onto calcite used as natural adsorbent, J. Hazard. Mater. 139 (3) (2007) 447–452.
- [7] G. Zhang, H. Liu, R. Liu, J. Qu, Removal of phosphate from water by a Fe-Mn binary oxide adsorbent, J. Colloid Interface Sci. 335 (2) (2009) 168–174.
- [8] J. Lu, H. Liu, R. Liu, X.u. Zhao, L. Sun, J. Qu, Adsorptive removal of phosphate by a nanostructured Fe–Al–Mn trimetal oxide adsorbent, Powder Technol. 233 (2013) 146–154
- [9] J. Xie, Z. Wang, S. Lu, D. Wu, Z. Zhang, H. Kong, Removal and recovery of phosphate from water by lanthanum hydroxide materials, Chem. Eng. J. 254 (2014) 163–170.
- [10] D. Zhao, A.K. Sengupta, Ultimate removal of phosphate from wastwater using a new class of polymeric ion exchangers, Water Res. 32 (1998) 1613–1625.
- [11] D. Petruzzelli, A. Dell'Erba, L. Liberti, M. Notarnicola, A.K. Sengupta, A phosphate-selective sorbent for the REM NUT® process: field experience at Massafra Wastewater Treatment Plant, React. Funct. Polym. 60 (2004) 195–202.
- [12] L. BLANEY, S. CINAR, A. SENGUPTA, Hybrid anion exchanger for trace phosphate removal from water and wastewater, Water Res. 41 (7) (2007) 1603–1613.
- [13] T. Nur, M.A.H. Johir, P. Loganathan, T. Nguyen, S. Vigneswaran, J. Kandasamy, Phosphate removal from water using an iron oxide impregnated strong base anion exchange resin, J. Ind. Eng. Chem. 20 (4) (2014) 1301–1307.
- [14] G.A. Maul, Y. Kim, A. Amini, Q. Zhang, T.H. Boyer, Efficiency and life cycle environmental impacts of ion-exchange regeneration using sodium, potassium, chloride, and bicarbonate salts, Chem. Eng. J. 254 (2014) 198–209.
- [15] L. Blaney, Nutrient extraction and recovery devices for isolation and separation of target products from animal produced waste streams. US patent, US20170174577A1 (expiration, March 7, 2037). 2016. https://extension.okstate. edu/fact-sheets/solids-content-of-wastewater-and-manure.html.
- [16] F.G. Donnan, Theory of membrane equilibria and membrane potentials in the presence of non-dialysing electrolytes, A contribution to physical-chemical physiology, Journal of Membrane Science 100 (1) (1995) 45–55.
- [17] E.H. Rotta, C.S. Bitencourt, L. Marder, A.M. Bernardes, Phosphorus recovery from low phosphate-containing solutions by electrodialysis, J. Membr. Sci. 573 (2019) 293–300.
- [18] Y. Zhang, E. Desmidt, A. Van Looveren, L. Pinoy, B. Meesschaert, B. Van der Bruggen, Phosphate separation and recovery from wastewater by novel electrodialysis, Environ. Sci. Technol. 47 (11) (2013) 5888–5895.
- [19] D. Hamilton, H. Zhang, Solids content of wastewater and manure, 2016. https://e xtension.okstate.edu/fact-sheets/solids-content-of-wastewater-and-manure.html.
- [20] A. TOR, Removal of fluoride from water using anion-exchange membrane under Donnan dialysis condition, J. Hazard. Mater. 141 (3) (2007) 814–818.
- [21] Q. Wang, J.J. Lenhart, H.W. Walker, Recovery of metal cations from lime softening sludge using Donnan dialysis, J. Membr. Sci. 360 (1-2) (2010) 469–475.
- [22] P. Prakash, A.K. Sengupta, Selective coagulant recovery from water treatment plant residuals using Donnan membrane principle, Environ. Sci. Technol. 37 (2003) 4468–4474, https://pubs.acs.org/doi/abs/10.1021/es030371q.
- [23] C. Chen, T. Dong, M. Han, J. Yao, L.e. Han, Ammonium recovery from wastewater by Donnan dialysis: A feasibility study, J. Cleaner Prod. 265 (2020) 121838, https://doi.org/10.1016/j.jclepro.2020.121838, https://www.sciencedirect. com/science/article/abs/pii/S0959652620318850.
- [24] L. Cumbal, A.K. Sengupta, Arsenic removal using polymer-supported hydrated iron oxide nanoparticles: Role of Donnan Membrane Effect, Environ. Sci. Technol. 39 (2005) 6508–6515.
- [25] A. Tor, Y. Çengeloğlu, M. Ersöv, G. Arslan, Transport of chromium through cationexchange membranes by Donnan dialysis in the presence of some metals of different valences, Desalination 170 (2) (2004) 151–159.
- [26] C. Agarwal, S. Chaudhury, A. Mhatre, A. Goswami, Donnan membrane equilibrium studies of mercury salts with Nafion-117 membrane, Desalin. Water Treat. 38 (1-3) (2012) 262–266.

- [27] O. Altintas, A. Tor, Y. Cengeloglu, M. Ersoz, Removal of nitrate from the aqueous phase by Donnan dialysis, Desalination 239 (1-3) (2009) 276–282.
- [28] I.M. Trifi, B. Trifi, S.B. Ayed, B. Hamrouni, Removal of phosphate by Donnan dialysis coupled with adsorption onto alginate calcium beads, Water Sci. Technol. 80 (1) (2019) 117–125.
- [29] M. Hichour, F. Persin, J. Sandeaux, C. Gavach, Fluoride removal from waters by Donnan dialysis, Sep. Purif. Technol. 18 (1) (1999) 1–11.
- [30] T. Turki, M. Ben Amor, Nitrate removal from natural water by coupling adsorption and Donnan dialysis. Water Sci, Technol. Water Supply 17 (2017) 771–779, https://iwaponline.com/ws/article/17/3/771/30660/Nitrate-removal-from-na tural-water-by-coupling.
- [31] S. Ring, D. Hasson, H. Shemer, R. Semiat, Simple modeling of Donnan separation processes, J. Membr. Sci. 476 (2015) 348–355.
- [32] M.M. Bejamin, Water chemistry, 2nd ed., Waveland Press, Incorporated, 2015.
- [33] P. Prakash, A.K. Sengupta, Selective coagulant recovery from water treatment plant residuals using Donnan membrane process, Environ. Sci. Technol. 37 (2003) 4468–4474, https://pubs.acs.org/doi/abs/10.1021/es030371q?casa_t oken=kZOZ3gINb7QAAAA:Zpxq0WRXL9ImyNbbvD8yLI_nRHmHYBCnCmt iSoogsmdMg1iFWDdxLcaxHaNGFGjlqlgnR0aNKkbKbYg.
- [34] Y. Çengeloğlu, A. Tor, E. Kir, M. Ersöz, Transport of hexavalent chromium through anion-exchange membranes, Desalination 154 (3) (2003) 239–246.
- [35] B. Etter, E. Tilley, R. Khadka, K.M. Udert, Low-cost struvite production using source-separated urine in Nepal, Water Res. 45 (2011) 852–862.
- [36] S.R. Sakthivel, E. Tilley, K.M. Udert, Wood ash as a magnesium source for phosphorus recovery from source-separated urine, Sci. Total Environ. 419 (2012) 68–75.
- [37] U. Shashvatt, J. Benoit, H. Aris, L. Blaney, CO2-assisted phosphorus extraction from poultry litter and selective recovery of struvite and potassium struvite, Water Res. 143 (2018) 19–27.
- [38] U. Shashvatt, H. Aris, L. Blaney, Evaluation of animal manure composition for protection of sensitive water supplies through nutrient recovery processes, Chemistry and Water (2017) 469–509.
- [39] F.G. Helfferich, Ion Exchange, Illustrated, Reprint ed., McGraw-Hill 1962. https://books.google.com/books/about/Ion Exchange.html?id=F9OQMEA88CAC.
- [40] R.E. Barron, J.S. Fritz, Effect of functional group structure and exchange capacity on the selectivity of anion exchangers for divalent anions, J. Chromatogr. 316 (1984) 201–210.
- [41] Y. Marcus, On water structure in concentrated salt solutions, J. Solution Chem. 38 (5) (2009) 513–516.
- [42] H. Kimura, Y. Yasaka, M. Nakahara, N. Matubayasi, Nuclear magnetic resonance study on rotational dynamics of water and benzene in a series of ionic liquids: anion and cation effects, J. Chem. Phys. 137 (2012), 194503.
- [43] K. Leung, S.B. Rempe, Ab initio molecular dynamics study of formate ion hydration, Journal of American Chemical Society 126 (1) (2004) 344–351.

- [44] J. Sun, D. Bousquet, H. Forbert, D. Marx, Glycine in aqueous solution: solvation shells, interfacial water, and vibrational spectroscopy from ab initio molecular dynamics, J. Chem. Phys. 133 (2010), 114508.
- [45] J. Israelachvili, Intermolecular forces and surface forces, 3rd ed., Academic Press,
- [46] J. Zhou, X. Lu, Y. Wang, J. Shi, Molecular dynamics study on ionic hydration, Fluid Phase Equilib. 194-197 (2002) 257–270.
- [47] L. Han, S. Galier, H, Roux-de Balmann, Ion hydration number and electro-osmosis during electrodialysis of mixed salt solution, Desalination 373 (2015) 38–46.
- [48] Brian J. Teppen, David M. Miller, Hydration energy determines isovalent cation exchange selectivity by clay minerals, Soil Sci. Soc. Am. J. 70 (1) (2006) 31–40.
- [49] David Hasson, Adam Beck, Fiana Fingerman, Chen Tachman, Hilla Shemer, Raphael Semiat, Simple model for characterizing a Donnan dialysis process, Ind. Eng. Chem. Res. 53 (14) (2014) 6094–6102.
- [50] Bin Zhao, Huazhang Zhao, Jinren Ni, Modeling of the Donnan dialysis process for arsenate removal, Chem. Eng. J. 160 (1) (2010) 170–175.
- [51] H. Miyoshi, Diffusion coefficients of ions throug ion-exchange membranes for Donnan dialysis using ions of the same valence, Chem. Eng. Sci. 52 (1996) 1087–1096.
- [52] Chhavi Agarwal, Sanhita Chaudhury, A.K. Pandey, A. Goswami, Kinetic aspects of Donnan dialysis through Nafion-117 membrane, J. Membr. Sci. 415-416 (2012) 681–685.
- [53] Hirofumi Miyoshi, Diffusion coefficients of ions through ion-exchange membranes for Donnan dialysis using ions of the same valence, Chem. Eng. Sci. 52 (7) (1997) 1087–1096.
- [54] A.L. Horvath, Handbook of aqueous electrolytes solutions: physical properties, estimation and correlation methods, Ellis Horwood series in Physical Chemistry, John Wiley and Sons, New York, 1985.
- [55] E.L. Cussler, Diffusion-mass transfer in fluid systems, Cambridge University Press, Cambridge, United Kingdom, 1984.
- [56] S. Mazrou, H. KerDjoudj, A.T. Cherif, Sodium hydroxide and hydrochloride acid generation from sodium chloride and rock salt by electro-electrodialysis, J. Appl. Electrochem. 27 (1997) 558–567.
- [57] E. Güler Akgemci, Mustafa Ersöz, Tevfik Atalay, Transport of formic acid through anion exchange membranes by Diffusion Dialysis and Electro-Electro Dialysis, Sep. Sci. Technol. 39 (1) (2005) 165–184.
- [58] T. Xue, R.B. Longwell, K. Osseo-Asare, Mass transfer in Nafion membrane systems: Effects of ionic size and charge on selectivity, J. Membr. Sci. 58 (1991) 175–189.
- [59] Jovan Kamcev, Benny D. Freeman, Cracks help membranes to stay hydrated, Nature 532 (7600) (2016) 445–446.
- [60] Gérald Pourcelly, Angeliki Oikonomou, Claude Gavach, H.D. Hurwitz, Influence of the water content on the kinetics of counter-ion transport in perfluorosulphonic membranes. J. Electroanal. Chem. 287 (1) (1990) 43–59.
- [61] R. Epsztein, E. Shaulsky, M. Qin, M. Elimelech, Activation behavior for ion permeation in ion-exchange membranes: Role of ion dehydration in selective transport, J. Membr. Sci. 580 (2019) 316–326.